SLAC-PUB-14942

UCHEP-09-02

B^+ and D_S^+ Decay Constants from Belle and Babar

A. J. Schwartz

Department of Physics, University of Cincinnati, P.O. Box 210011, Cincinnati, Ohio 45221

Abstract. The Belle and Babar experiments have measured the branching fractions for $B^+ \to \tau^+ \nu$ and $D_s^+ \to \mu^+ \nu$ decays. From these measurements one can extract the B^+ and D_s^+ decay constants, which can be compared to lattice QCD calculations. For the D_s^+ decay constant, there is currently a 2.1σ difference between the calculated value and the measured value.

Keywords: leptonic decays, decay constants, lattice QCD
PACS: 12.15.Hh,13.20.He

INTRODUCTION

Both the Belle [1] and Babar [2] experiments have measured the branching fractions for $B^+ \to \tau^+ \nu$ and $D_s^+ \to \mu^+ \nu$ decays [3]. These decays proceed via the annihilation diagram of Fig. 1. Within the Standard Model (SM), the predicted rates are

$$\mathscr{B}(B^+ \to \tau^+ \nu) = \tau_{B^+} \frac{G_F^2}{8\pi} |V_{ub}|^2 f_{B^+}^2 m_\tau^2 m_{B^+} \left(1 - \frac{m_\tau^2}{m_{B^+}^2}\right)^2 \quad (1)$$

$$\mathscr{B}(D_s^+ \to \ell^+ \nu) = \tau_{D_s} \frac{G_F^2}{8\pi} |V_{cs}|^2 f_{D_s}^2 m_\ell^2 m_{D_s} \left(1 - \frac{m_\ell^2}{m_{D_s}^2}\right)^2 . \quad (2)$$

For the D_s^+, all parameters on the right-hand-side except for f_{D_s} are well-known. The Cabibbo-Kobayashi-Maskawa (CKM) matrix element $|V_{cs}|$ is well-constrained by a global fit to several experimental observables and unitarity of the CKM matrix. Thus a measurement of $\mathscr{B}(D_s^+ \to \mu^+ \nu)$ allows one to determine the decay constant f_{D_s}. This can be compared to QCD lattice calculations, which have become relatively precise. For the B^+, the CKM matrix element $|V_{ub}|$ is known to only 9%; this is nonetheless more precise than measurements of $\mathscr{B}(B^+ \to \ell^+ \nu)$ and allows one to extract f_B.

MEASUREMENT OF $B^+ \to \tau^+ \nu$

Belle has done two $B^+ \to \tau^+ \nu$ analyses [4, 5]; the most recent one used 605 fb^{-1} of data and obtained evidence for a signal. This analysis employed a semileptonic tag: one B in an event is fully reconstructed as $B^- \to D^{(*)0} \ell^- \bar{\nu}$, where $D^{*0} \to D^0 \pi^0$, $D^0 \gamma$ and $D^0 \to K^- \pi^+ (\pi^0), K^- \pi^+ \pi^- \pi^+$. The signal decays $\tau^+ \to \mu^+ \nu_\mu \bar{\nu}_\tau$, $e^+ \nu_e \bar{\nu}_\tau$ and $\tau^+ \to \pi^+ \bar{\nu}_\tau$ are then searched for by reconstructing a single track not associated with the tag side. The signal yield is obtained by fitting the distribution of $E_{\rm ECL}$, which is the energy sum of

Work supported in part by US Department of Energy contract DE-AC02-76SF00515.

SLAC National Accelerator Laboratory, Menlo Park, CA 94025

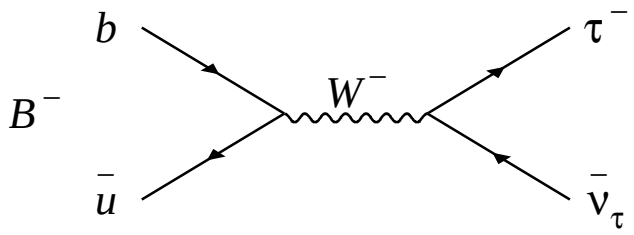

FIGURE 1. Annihilation diagram for a heavy meson decaying to a lepton and neutrino.

TABLE 1. Fit results for $B^+ \to \tau^+ \nu$, from Belle [5]. The data sample corresponds to 605 fb^{-1}.

Decay Mode	Signal Yield	ε (%)	$\mathscr{B} \times 10^4$
$\tau^- \to e^- \bar{\nu} \nu_\tau$	78^{+23}_{-22}	0.059	$2.02^{+0.59}_{-0.56}$
$\tau^- \to \mu^- \bar{\nu} \nu_\tau$	15^{+18}_{-17}	0.037	$0.62^{+0.76}_{-0.71}$
$\tau^- \to \pi^- \nu_\tau$	58^{+21}_{-20}	0.047	$1.88^{+0.70}_{-0.66}$
Combined	154^{+36}_{-35}	0.143	$1.65^{+0.38}_{-0.37}$

calorimeter clusters not associated with a charged track. A peak near $E_{\rm ECL} = 0$ indicates a $\tau^+ \to \ell^+ \nu_\ell \bar{\nu}_\tau$ or $\tau^+ \to \pi^+ \bar{\nu}_\tau$ decay. The main backgrounds are $b \to c$ processes and $e^+e^- \to q\bar{q}$ continuum events. The fit is unbinned and uses a likelihood function

$$\mathscr{L} \;=\; \frac{e^{-\sum_j n_j}}{N!} \prod_i \sum_j n_j \, f_j(E_i)\,, \tag{3}$$

where i runs over all events (N), j runs over all signal and background categories, n_j is the yield of category j, and f_j is the probability density function (PDF) for category j. The branching fraction is calculated as $\mathscr{B} = n_s/(2 \cdot \varepsilon \cdot N_{B^+B^-})$, where ε is the reconstruction efficiency as calculated from Monte Carlo (MC) simulation. The fit results are listed in Table 1, and the fit projections are shown in Fig. 2. The systematic errors are dominated by uncertainty in the background PDF and the tag reconstruction efficiency. The overall result is

$$\mathscr{B}(B^+ \to \tau^+ \nu)\Big|_{\rm Belle} \;=\; \left(1.65^{+0.38\,+0.35}_{-0.37\,-0.37}\right) \times 10^{-4}\,, \tag{4}$$

where the first error is statistical and the second is systematic.

Babar has published two analyses of $B^+ \to \tau^+ \nu$ decays: one using a semileptonic tag [6] and the other using a hadronic tag [7]. Both analyses use data samples consisting of 383×10^6 $B\overline{B}$ pairs. The former is similar to that used in the Belle analysis: the tag side is reconstructed as $B^- \to D^{(*)0} \ell^- \bar{\nu}_\ell$, where $D^{*0} \to D^0\pi^0, D^0\gamma$ and $D^0 \to K^-\pi^+(\pi^0), K^-\pi^+\pi^-\pi^+, K_S\pi^+\pi^-$. Babar searches for $\tau^+ \to \ell^+ \nu_\ell \bar{\nu}_\tau$, $\tau^+ \to \pi^+ \bar{\nu}_\tau$, and also $\tau^+ \to \pi^+\pi^0 \bar{\nu}_\tau$, where for the last mode the $\pi^+\pi^0$ mass is required to be near that of the ρ^+. The signal is identified by plotting $E_{\rm extra}$, the energy sum of calorimeter clusters not associated with a charged track; a peak near zero indicates τ^+ decay. The

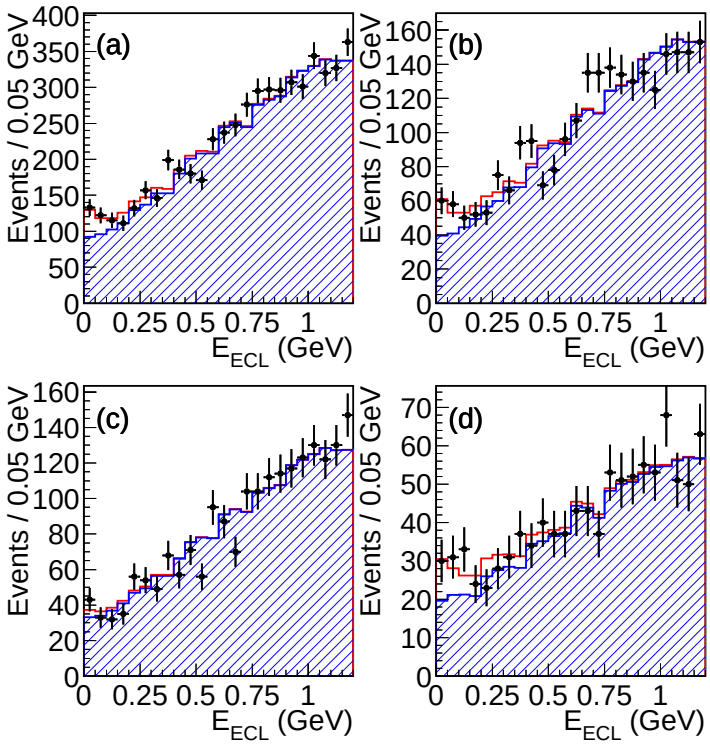

FIGURE 2. E_{ECL} distribution of data events (points) and fit projections for $B^+ \to \tau^+ \nu$, from Belle [5]. *(a)* all τ decay modes combined; *(b)* $\tau^- \to e^- \bar{\nu}_e \nu_\tau$; *(c)* $\tau^- \to \mu^- \bar{\nu}_\mu \nu_\tau$; *(d)* $\tau^- \to \pi^- \nu_\tau$. The open and hatched histograms correspond to signal and background, respectively.

signal yield is obtained by counting events in a signal region, e.g., $E_{\rm extra} < 0.50$, and subtracting off background as estimated from $E_{\rm extra}$ sidebands. The number of events in the final sample is 245, the background estimate is 222 ± 13, and the resulting branching fraction is $(0.9 \pm 0.6\ (\text{stat.}) \pm 0.1\ (\text{syst.})) \times 10^{-4}$.

The Babar hadronic-tag analysis is more complicated. The tagging side is reconstructed as $B^- \to D^{(*)0} X^-$, where X^- denotes a hadronic system of total charge -1 composed of $n_1(\pi^\pm)$, $n_2(K^\pm)$, $n_3(K^0_S)$, and $n_4(\pi^0)$, where $n_1 + n_2 \leq 5$, $n_3 \leq 2$, and $n_4 \leq 2$. The $D^{(*)0}$ is reconstructed in the same channels as those used for the semileptonic analysis, as is the τ^+ on the signal side. A background subtraction is done on the tag side. The signal yield is obtained by counting events in an $E_{\rm extra}$ signal region and subtracting off background as estimated from an $E_{\rm extra}$ sideband. There are 24 signal candidates and 14.3 ± 3.0 estimated background events; the resulting branching fraction is $(1.8^{+0.9}_{-0.8} \pm 0.4 \pm 0.2) \times 10^{-4}$, where the first error is statistical, the second is due to the background uncertainty, and the third is due to other systematic sources. The data is shown in Fig. 3 along with projections of the fit. This result is consistent with the

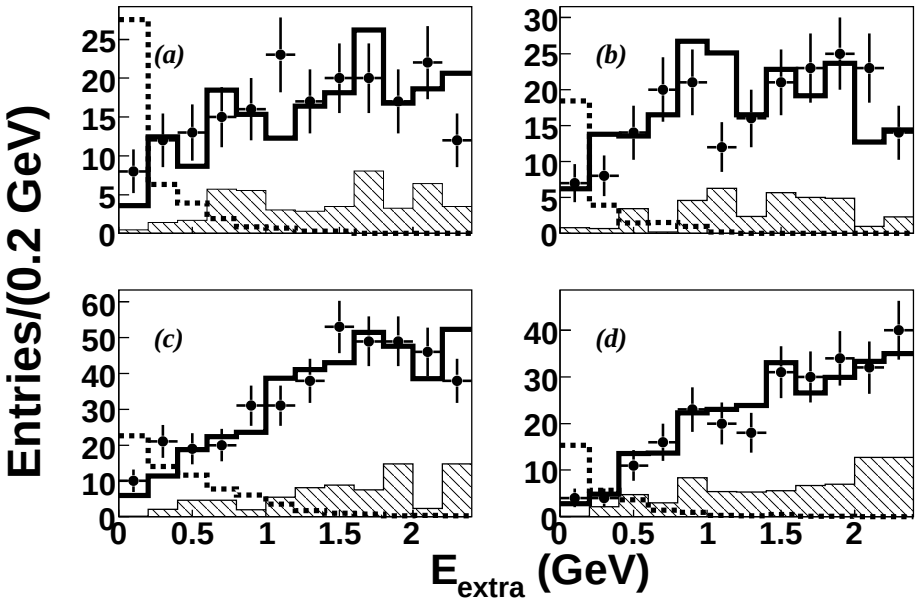

FIGURE 3. $E_{\rm extra}$ distribution of data events (points) and fit projections for $B^+ \to \tau^+ \nu$, from Babar using a hadronic tag [7]. *(a)* $\tau^- \to e^- \bar{\nu}_e \nu_\tau$; *(b)* $\tau^- \to \mu^- \bar{\nu}_\mu \nu_\tau$; *(c)* $\tau^- \to \pi^- \nu_\tau$; *(d)* $\tau^- \to \pi^- \pi^0 \nu_\tau$. The hatched histogram shows the combinatorial background component, and, for comparison, the open histogram shows $B^+ \to \tau^+ \nu$ signal for a branching fraction of 0.3%.

semileptonic-tagged result; combining the two gives

$$\mathscr{B}(B^+ \to \tau^+ \nu)\Big|_{\rm Babar} \;=\; \Big(1.2 \pm 0.4\,(\text{stat.}) \pm 0.3\,(\text{bkg.}) \pm 0.2\,(\text{syst.})\Big) \times 10^{-4}\,. \quad (5)$$

This is consistent with the Belle result, Eq. (4).

MEASUREMENT OF $D_s^+ \to \mu^+ \nu$

The Belle analysis of $D_s^+ \to \mu^+ \nu$ decays [8] uses 548 fb^{-1} of data and searches for $e^+e^- \to DKD_s^* n(\pi,\gamma)$, where the primary D and K can be charged or neutral; the D_s^* is "reconstructed" (see below) via $D_s^+\gamma$; $n(\pi,\gamma) \equiv X$ signifies any number of additional pions and up to one photon (from fragmentation); the D is reconstructed via $D \to K\, n(\pi)$, where $n = 1,2,3$; and neutral kaons are reconstructed via $K_S^0 \to \pi^+\pi^-$. If the primary K is charged, both it and the D must have flavors opposite to that of the D_s^+; these constitute a "right-sign" (RS) sample. If the flavors are not both opposite, the event is categorized as "wrong-sign" (WS) and used to parameterize the background. The same classification applies to primary neutral K events, except for these only the D flavor must be opposite to that of the D_s^+ for the event to be classified as RS.

The decay sequence is identified via a recoil mass technique. First, the recoil mass of the D, K, and X particles is calculated and required to be within 150 MeV/c^2 of $M_{D_s^*}$; then the γ is included and the recoil mass is required to be within 150 MeV/c^2 of $M_{D_s^+}$;

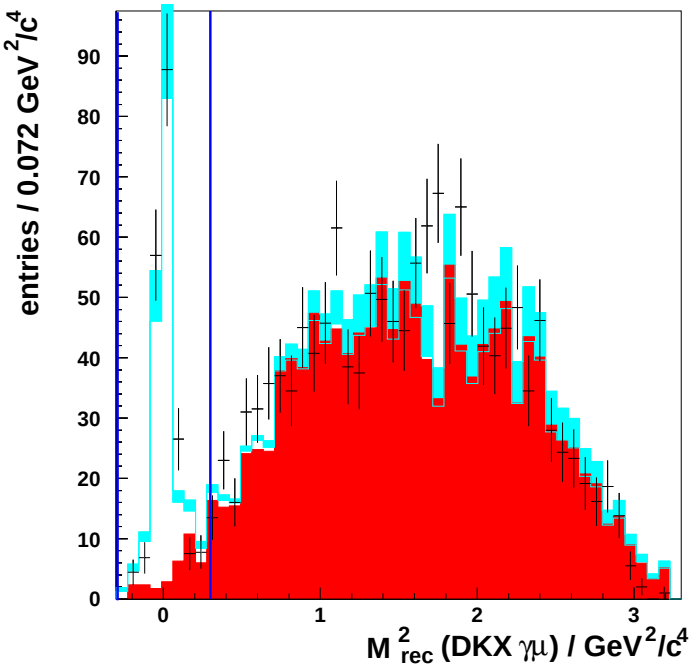

FIGURE 4. Recoil mass distribution for $e^+e^- \to DKX\gamma\mu^+$, from Belle [8].

and finally, the μ^+ is included and the recoil mass required to be within 0.55 GeV/c^2 of zero. The final $DKX\gamma\mu^+$ recoil mass distribution is shown in Fig. 4; a sharp peak is observed near zero, indicating $D_s^+ \to \mu^+\nu$ decay.

The analysis is complicated by the fact that the recoil mass technique is very sensitive to the number of tracks in an event and the track reconstruction efficiency, as all tracks must be reconstructed for the recoil mass to be accurate. As it is difficult to simulate track multiplicity accurately due to uncertainties in quark fragmentation, the data is divided into bins of n_x^R, the number of "primary particles" reconstructed in an event. Here, a primary particle is one that is not a daughter of any particle reconstructed in the event. The minimum value for n_x^R is three, corresponding to $e^+e^- \to DKD_s^*$ without any additional particles from fragmentation. The data is then fit in two dimensions, $DKX\gamma$ recoil mass vs. n_x^R (see Fig. 5). The signal PDF is obtained from MC and modeled separately for different values of n_x^T, the *true* number of primary particles in an event (n_x^T can differ from n_x^R due to particles being lost or incorrectly assigned).

The branching fraction is obtained from two fits: the first fit uses the $DKX\gamma$ recoil mass spectrum and yields the number of D_s^+ candidates; the result is $N_{D_s} = 32100 \pm 870\,(\text{stat}) \pm 1210\,(\text{syst})$. For this fit the background shape is taken from the WS sample and the background levels floated in the fit. The second fit uses the $DKX\gamma\mu^+$ recoil mass spectrum and yields the number of $D_s^+ \to \mu^+\nu$ candidates; the result is $N_{\mu\nu} = 169 \pm 16\,(\text{stat}) \pm 8\,(\text{syst})$. For this fit the background shape is taken from a RS "$D_s^+ \to e^+\nu$" sample, i.e., all selection criteria are the same except that an electron candidate is required instead of a muon candidate. As true $D_s^+ \to e^+\nu$ decays are suppressed by $\sim 10^{-5}$, this sample provides a good model of the $D_s^+ \to \mu^+\nu$ background. The

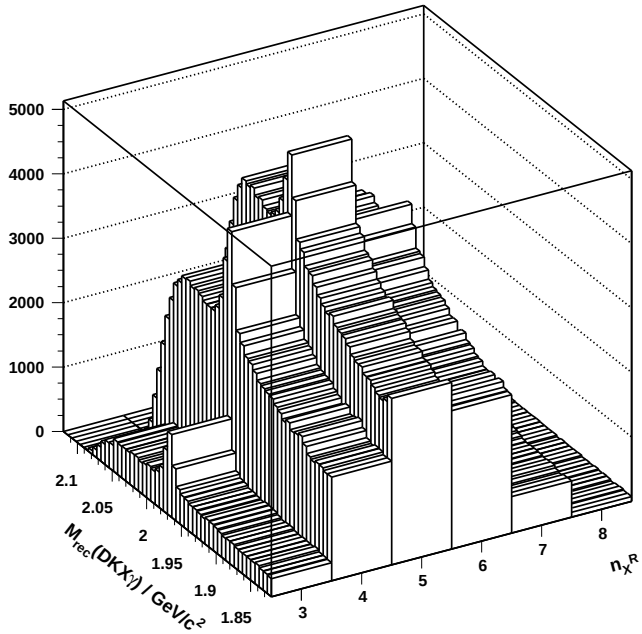

FIGURE 5. Two-dimensional $DKX\gamma$ recoil mass vs. n_x^R distribution (see text), from Belle [8].

systematic errors listed are dominated by uncertainties in the signal and background PDFs and are obtained by varying the shapes of these PDFs. The branching fraction is the ratio $N_{\mu\nu}/N_{D_s}$, corrected for the ratio of reconstruction efficiencies. The result is

$$\mathscr{B}(D_s^+ \to \mu^+\nu)\Big|_{\text{Belle}} \;=\; \Big(6.44 \pm 0.76\ (\text{stat.}) \pm 0.57\ (\text{syst.})\Big) \times 10^{-3}. \qquad (6)$$

The Babar experiment searches for $D_s^+ \to \mu^+\nu$ [9] using 230 fb^{-1} of data by fully reconstructing a flavor-specific $D^{(*)-}$, $\overline{D}^0$, or D_s^- decay on the tagging side. Tag candidates are reconstructed in the following modes: $\overline{D}^0 \to K^+\pi^-(\pi^0), K^+\pi^-\pi^+\pi^-$; $D^- \to K^+\pi^-\pi^-(\pi^0), K_S^0\pi^-(\pi^0), K_S^0\pi^-\pi^-\pi^+, K^+K^-\pi^-, K_S^0K^-$; $D_s^- \to K_S^0K^-, \phi\rho^-$; and $D^{*-} \to \overline{D}^0\pi^-$ with $\overline{D}^0 \to K_S^0\pi^+\pi^-(\pi^0), K_S^0K^+K^-, K_S^0\pi^0$. An isolated μ^+ track is required. The neutrino momentum is taken to be the missing momentum in the event: $\vec{p}_\nu \equiv \vec{p}_{e^+e^-} - \vec{p}_{\text{rest}}$. A photon is required and paired with the D_s^+ candidate to make a D_s^{*+}, and the mass difference $\Delta M \equiv M(\mu^+\nu\gamma) - M(\mu^+\nu)$ is calculated.

The data is subsequently divided into four subsamples: a tag-side mass sideband and a tag-side signal region for μ^+ and e^+ candidates. For both lepton samples, the tag-side-sideband ΔM spectrum is subtracted from the tag-side-signal ΔM spectrum (Fig. 6), and then the sideband-subtracted e^+ spectrum is subtracted from the sideband-subtracted μ^+ spectrum. The final ΔM distribution (Fig. 7a) is fit with signal and background PDFs; the signal yield obtained is $N_{\mu^+\nu} = 489 \pm 55$ events.

To determine the branching fraction, the signal yield is normalized to $D_s^+ \to \phi\pi^+$ decays. Like the signal mode, the D_s^+ candidate is required to originate from $D_s^{*+} \to D_s^+\gamma$.

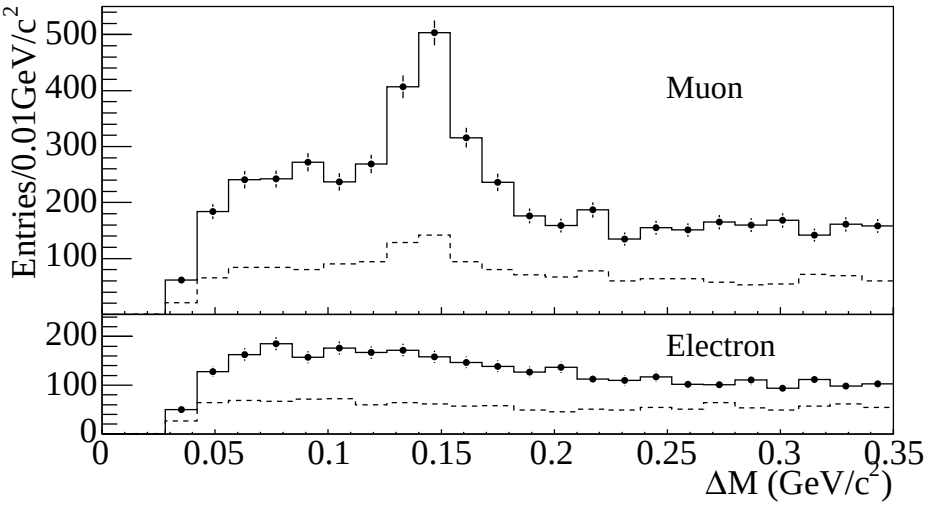

FIGURE 6. ΔM spectra for the tag-side sideband region (dashed) and tag-side signal region (solid) for μ^+ (top) and e^+ (bottom) samples, from Babar [9].

The tag-side-sideband ΔM spectrum is subtracted from the tag-side-signal ΔM spectrum, and the resulting spectrum is fit with signal and background PDFs (Fig. 7b). The signal yield obtained is $N_{\phi\pi^+} = 2093 \pm 99$ events. Dividing $N_{\mu^+\nu}$ by $N_{\phi\pi^+}$ and correcting for the ratio of reconstruction efficiencies gives

$$\left.\frac{\Gamma(D_s^+ \to \mu^+\nu)}{\Gamma(D_s^+ \to \phi\pi^+)}\right|_{\text{Babar}} = 0.143 \pm 0.018\ (\text{stat.}) \pm 0.006\ (\text{syst.}). \quad (7)$$

For this analysis, the ϕ is reconstructed via $\phi \to K^+K^-$ with $|M_{K^+K^-} - M_\phi| \equiv \Delta M_{KK} <$ 5.5 MeV [10]. Conveniently, CLEO has measured the branching fraction $\mathscr{B}(D_s^+ \to K^+K^-\pi^+)$ for $\Delta M_{KK} = 5$ MeV; the result is $(1.69 \pm 0.08 \pm 0.06)\%$ [11]. To multiply the two results together to obtain $\mathscr{B}(D_s^+ \to \mu^+\nu)$ requires dividing Eq. (7) by $\mathscr{B}(\phi \to K^+K^-) = 0.491$ and subtracting (in quadrature) the 1.2% uncertainty in $\mathscr{B}(\phi \to K^+K^-)$ from the systematic error. In addition, Babar has subtracted off a small amount of $D_s^+ \to f_0(980)(K^+K^-)\pi^+$ background (48 events); as this process is included in the CLEO measurement, these events must be added back in to Babar's $\phi\pi^+$ yield. Thus the Babar result becomes

$$\left.\frac{\Gamma(D_s^+ \to \mu^+\nu)}{\Gamma(D_s^+ \to K^+K^-\pi^+)}\right|_{\Delta M_{KK}=5.5\text{ MeV}} = 0.285 \pm 0.035\ (\text{stat.}) \pm 0.011\ (\text{syst.}). \quad (8)$$

Multiplying this by CLEO's measurement gives

$$\mathscr{B}(D_s^+ \to \mu^+\nu)\Big|_{\text{Babar}} = \Big(4.81 \pm 0.63\ (\text{stat.}) \pm 0.25\ (\text{syst.})\Big) \times 10^{-3}. \quad (9)$$

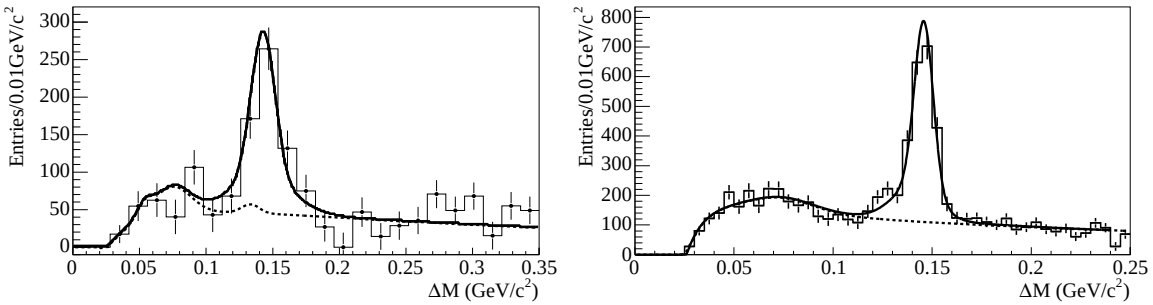

FIGURE 7. Background-subtracted ΔM spectra (see text) and projections of the fit result, from Babar [9]. The left-most (right-most) distribution corresponds to $D_s^+ \to \mu^+\nu$ ($D_s^+ \to \phi\pi^+$) candidates. The dashed line is the background component, and the solid line is the signal plus background components combined.

EXTRACTION OF DECAY CONSTANTS

The Belle and Babar collaborations have used their measurements of $\mathscr{B}(B^+ \to \tau^+\nu)$ and Eq. (1) to calculate the product of the B decay constant f_B and the CKM matrix element $|V_{ub}|$. The results are

$$f_B \times |V_{ub}| \times 10^4 \;=\; \begin{cases} 9.7 \pm 1.1\ (\text{stat.})\, ^{+1.0}_{-1.1}\ (\text{syst.})\ \text{GeV} \quad (\text{Belle}) \\ 7.2\, ^{+2.0}_{-2.8}\ (\text{stat.}) \pm 0.2\ (\text{syst.})\ \text{GeV} \quad (\text{Babar semileptonic}) \\ 10.1\, ^{+2.3}_{-2.5}\ (\text{stat.})\, ^{+1.2}_{-1.5}\ (\text{syst.})\ \text{GeV} \quad (\text{Babar hadronic}). \end{cases}$$

Taking a weighted average gives

$$f_B \times |V_{ub}|_{\,(\text{Belle+Babar avg.})} \;=\; (9.2 \pm 1.2) \times 10^{-4}\ \text{GeV}, \tag{10}$$

and dividing by the Particle Data Group value $|V_{ub}| = (0.393 \pm 0.036)\%$ [12] gives

$$f_B\big|_{(\text{Belle+Babar avg.})} \;=\; 233 \pm 37\ \text{MeV}. \tag{11}$$

This value is 1σ higher than the most recent lattice QCD results, that of the HPQCD collaboration (190 ± 13 MeV [13]) and that of the Fermilab/MILC collaboration (195 ± 11 MeV [14]).

The Heavy Flavor Averaging Group (HFAG) has calculated a world average (WA) value for $\mathscr{B}(D_s^+ \to \mu^+\nu)$ and used this to determine a WA value for the D_s^+ decay constant f_{D_s} [15]. This value can be compared to recent lattice QCD calculations; a significant difference could indicate new physics. The WA value for f_{D_s} is obtained by inverting Eq. (2):

$$f_{D_s} \;=\; \frac{1}{G_F |V_{cs}| m_\ell \left(1 - \dfrac{m_\ell^2}{m_{D_s}^2}\right)} \sqrt{\frac{8\pi\, \mathscr{B}(D_s^+ \to \ell^+\nu)}{m_{D_s}\, \tau_{D_s}}}, \tag{12}$$

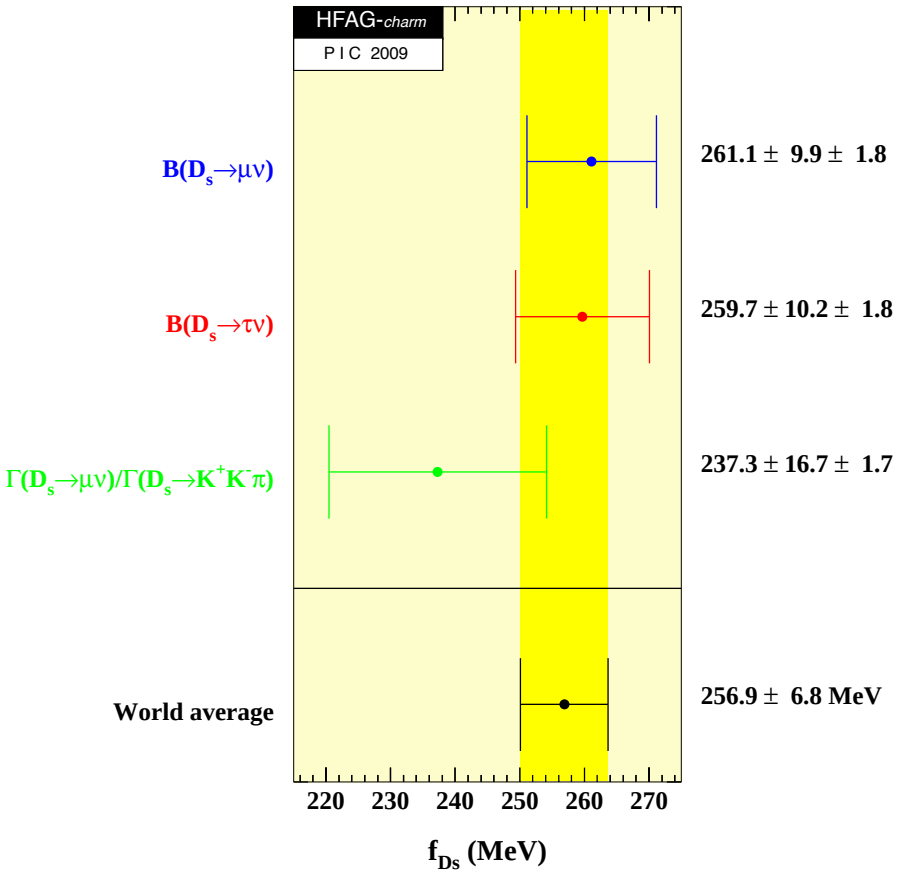

FIGURE 8. Heavy Flavor Averaging Group (HFAG) WA value for f_{D_s}, from Ref. [15]. For each measurement, the first error listed is the total uncorrelated error, and the second error is the total correlated error (mostly from τ_{D_s}).

where, for $\mathscr{B}(D_s^+ \to \ell^+ \nu)$, the WA value is inserted. The error on f_{D_s} is calculated as follows: values for variables on the right-hand-side of Eq. (12) are sampled from Gaussian distributions having means equal to the central values and standard deviations equal to their respective errors. The resulting values of f_{D_s} are plotted, and the distribution is fit to a bifurcated Gaussian to obtain the $\pm 1\sigma$ errors.

The results of this procedure are shown in Fig. 8. Also included are measurements of $\mathscr{B}(D_s^+ \to \mu^+ \nu)$ [16] and $\mathscr{B}(D_s^+ \to \tau^+ \nu)$ [17] from CLEO. Thus there are three types of measurements: f_{D_s} from the absolute $D_s^+ \to \mu^+ \nu$ branching fraction, f_{D_s} from the absolute $D_s^+ \to \tau^+ \nu$ branching fraction, and f_{D_s} from the $\Gamma(D_s^+ \to \mu^+ \nu)/\Gamma(D_s^+ \to K^+ K^- \pi^+)$ ratio. The overall WA value is obtained by averaging the three results, carefully accounting for correlations such as the input values for $|V_{cs}|$ and τ_{D_s}. The result is 256.9 ± 6.8 MeV. This value is higher than the two most precise lattice QCD results, that of the HPQCD (241 ± 3 MeV [18]) and Fermilab/MILC (249 ± 11 MeV [14]) collaborations. The weighted average of the theory results is 241.5 ± 2.9 MeV, which differs from the HFAG result by 2.1σ.

SUMMARY

In summary, Belle has observed $B^+ \to \tau^+ \nu$ with 3.8σ significance. From the measured branching fraction they determine the product $f_B \times |V_{ub}|$. Babar has observed $B^+ \to \tau^+ \nu$ with 2.6σ significance and has also measured the branching fraction to determine $f_B \times |V_{ub}|$. The results from the two experiments are consistent; the weighted average has 13% precision and is consistent with lattice QCD calculations.

For $D_s^+ \to \mu^+ \nu$ decays, Belle has observed this mode using a recoil mass technique and has measured the branching fraction with 15% precision. Babar has also observed this mode and has measured the branching fraction relative to that for $D_s^+ \to \phi\pi^+$ with 13% precision. Dividing this by the branching fraction for $\phi \to K^+K^-$ and including $D_s^+ \to f_0(980)(K^+K^-)\pi^+$ decays allows one to multiply by CLEO's measurement of $\mathscr{B}(D_s^+ \to K^+K^-\pi^+)$ to obtain $\mathscr{B}(D_s^+ \to \mu^+\nu)$. The Heavy Flavor Averaging Group has used the Belle and Babar measurements and also measurements from CLEO to calculate a world average value for f_{D_s}; the result is 256.9 ± 6.8 MeV. This value is 2.1σ higher than the average of two recent lattice QCD calculations; the difference could indicate new physics.

ACKNOWLEDGMENTS

We thank the organizers of CIPANP 2009 for a stimulating scientific program and excellent hospitality. We thank Laurenz Widhalm, Yoshihide Sakai, and Andreas Kronfeld for reviewing this manuscript and suggesting many improvements.

REFERENCES

1. Belle experiment, `http://belle.kek.jp/`.
2. Babar experiment, `http://www.slac.stanford.edu/BFROOT/`.
3. Unless noted otherwise, charge-conjugate modes are implicitly included.
4. K. Ikado *et al.* (Belle Collab.), *Phys. Rev. Lett.* **97**, 251802 (1996).
5. I. Adachi *et al.* (Belle Collab.), arXiv:0809.3834.
6. B. Aubert *et al.* (Babar Collab.), *Phys. Rev. D* **76**, 052002 (2007). A preliminary (unpublished) result with 20% more data is presented in B. Aubert *et al.* (Babar Collab.), arXiv:0809.4027.
7. B. Aubert *et al.* (Babar Collab.), *Phys. Rev. D* **77**, 011107 (2008).
8. R. Widhalm *et al.* (Belle Collab.), *Phys. Rev. Lett.* **100**, 241801 (2008).
9. B. Aubert *et al.* (Babar Collab.), *Phys. Rev. Lett.* **98**, 141801 (2007).
10. J. Coleman (Babar), private communication.
11. J. P. Alexander *et al.* (CLEO Collab.), *Phys. Rev. Lett.* **100**, 161804 (2008).
12. C. Amsler *et al.* (Particle Data Group), *Phys. Lett. B* **667**, 1 (2008) and 2009 partial update for the 2010 edition (`http://pdg.lbl.gov`).
13. E. Gámiz *et al.* (HPQCD Collab.), *Phys. Rev. D* **80** 014503 (2009).
14. C. Bernard *et al.* (Fermilab/MILC Collab.), arXiv:0904.1895.
15. Heavy Flavor Averaging Group (HFAG), `http://www.slac.stanford.edu/xorg/hfag/charm/index.html`.
16. J. P. Alexander *et al.* (CLEO Collab.), *Phys. Rev. D* **79** 052001 (2009).
17. J. P. Alexander *et al.* (CLEO Collab.), *Phys. Rev. D* **79** 052001 (2009).
    P. Onyisi *et al.* (CLEO Collab.), *Phys. Rev. D* **79** 052002 (2009).
18. E. Follana *et al.* (HPQCD Collab.), *Phys. Rev. Lett.* **100**, 062002 (2008).